N-terminal polyubiquitination and degradation of the Arf tumor suppressor

Mei-Ling Kuo,[1,3] Willem den Besten,[1,3] David Bertwistle,[1,2] Martine F. Roussel,[1] and Charles J. Sherr[1,2,4]

[1]Department of Genetics and Tumor Cell Biology and [2]Howard Hughes Medical Institute, St. Jude Children's Research Hospital, Memphis, Tennessee 38105, USA

Unknown mechanisms govern degradation of the p19^{Arf} tumor suppressor, an activator of p53 and inhibitor of ribosomal RNA processing. Kinetic metabolic labeling of cells with [^{3}H]-leucine indicated that p19^{Arf} is a relatively stable protein (half-life ~6 h) whose degradation depends upon the ubiquitin–proteasome pathway. Although p19^{Arf} binds to the Mdm2 E3 ubiquitin protein ligase to activate p53, neither of these molecules regulates p19^{Arf} turnover. In contrast, the nucleolar protein nucleophosmin/B23, which binds to p19^{Arf} with high stoichiometry, retards its turnover, and Arf mutants that do not efficiently associate with nucleophosmin/B23 are unstable and functionally impaired. Mouse p19^{Arf}, although highly basic (22% arginine content), contains only a single lysine residue absent from human p14^{ARF}, and substitution of arginine for lysine in mouse p19^{Arf} had no effect on its rate of degradation. Mouse p19^{Arf} (either wild-type or lacking lysine) and human p14^{ARF} undergo N-terminal polyubiquitination, a process that has not as yet been documented in naturally occurring lysine-less proteins. Re-engineering of the p19^{Arf} N terminus to provide consensus sequences for N-acetylation limited Arf ubiquitination and decelerated its turnover.

[*Keywords*: Arf tumor suppressor; proteasome; ubiquitin; nucleophosmin/B23; p53; Mdm2]

Supplemental material is available at http://www.genesdev.org.

Received April 21, 2004; revised version accepted June 7, 2004.

The Arf tumor suppressor protein (p19^{Arf} in the mouse, and p14^{ARF} in humans) antagonizes the functions of the p53-negative regulator Mdm2 to trigger p53-dependent cell-cycle arrest or apoptosis (Sherr 2001). Arf also has additional activities that are p53-independent, including an ability to inhibit ribosomal RNA (rRNA) processing (Sugimoto et al. 2003) and effects on gene expression (Eymin et al. 2001; Fatyol and Szalay 2001; Martelli et al. 2001; Datta et al. 2002; Kuo et al. 2003; Rocha et al. 2003). The p19^{Arf} protein is unusual in several respects. It is encoded by the *Ink4a* locus (now designated *Ink4a/Arf*; Quelle et al. 1995), which also specifies a totally unrelated polypeptide, p16^{Ink4a}, a potent inhibitor of cyclin D-dependent kinases (Serrano et al. 1993). Two transcripts initiated at separate promoters incorporate sequences from different first exons (1α and 1β) that are spliced to the products of a common downstream exon translated in alternative reading frames (from which Arf gets its name). Mouse p19^{Arf} is a basic protein containing ~22% arginine but only a single lysine residue that is not conserved in human p14^{ARF}. Given its basic nature, p19^{Arf} must be "buffered" by binding to other cellular proteins and/or nucleic acids. Most Arf protein localizes within the nucleolus where it is bound in complexes of high molecular mass (2–5 MDa) that include many other proteins (Weber et al. 1999; Bertwistle et al. 2004). Among the latter is nucleophosmin (NPM or B23), an abundant cellular protein which binds to p19^{Arf} with high stoichiometry (Itahana et al. 2003; Bertwistle et al. 2004).

Expression of *Arf* transcripts is difficult to detect in developing mouse embryos (Zindy et al. 1997), and mice lacking the gene develop normally but are highly prone to tumor formation (Kamijo et al. 1997). The levels of p19^{Arf} expressed in normal tissues in vivo are also quite low. *Arf* is induced by elevated and sustained oncogenic signals, such as those resulting from *Myc* overexpression (Zindy et al. 1998) or *Ras* mutation (Palmero et al. 1998) but not directly by other genotoxic stresses that lead to p53 stabilization. Studies using reporter mice in which a gene encoding green fluorescent protein (GFP) was substituted for *Arf* exon 1β have implied that *Arf* activation in vivo can efficiently eliminate incipient tumor cells (Zindy et al. 2003).

The p19^{Arf} protein progressively accumulates when primary mouse embryo fibroblasts (MEFs) are passaged in culture, correlating with their decreasing proliferative capacity and eventual senescence. In contrast, *Arf*-null MEFs continue to proliferate much like established cell

[3]**These authors contributed equally to this work.**
[4]**Corresponding author.**
E-MAIL sherr@stjude.org; FAX (901) 495-2381.
Article and publication are at http://www.genesdev.org/cgi/doi/10.1101/gad.1213904.

lines (Kamijo et al. 1997). Although one might imagine that $p19^{Arf}$ accumulation in senescing primary cells need not be accompanied by appreciable degradation, the mechanisms that regulate Arf turnover have not been elucidated. We show here that $p19^{Arf}$ is subject to more dynamic controls than previously thought, being degraded by the proteasome following N-terminal polyubiquitination.

Results

Turnover of $p19^{Arf}$ does not depend upon p53 or Mdm2

Because $p19^{Arf}$ contains a single internal methionine residue, pulse-chase analysis with [^{35}S]-methionine is problematic. Induced MT-Arf cells, an NIH-3T3 cell derivative lacking the endogenous *Ink4a-Arf* locus but engineered to synthesize HA-tagged $p19^{Arf}$ under control of the zinc-responsive metallothionein promoter (Kuo et al. 2003), were metabolically labeled with [^{3}H]-leucine and chased for various periods of time. Immunoprecipitated $p19^{Arf}$ resolved on denaturing gels was visualized by radiofluorography. The half-life ($t_{½}$) of $p19^{Arf}$ was found to be ~6 h (Fig. 1A; see below), consistent with a study in which human $p14^{ARF}$ degradation was monitored in cells treated with a protein synthesis inhibitor (Pollice et al. 2004).

Because p53 negatively regulates *Arf* gene expression (Kamijo et al. 1998; Stott et al. 1998), we performed similar analyses using proliferating *p53*-null MEFs that express relatively high levels of endogenous $p19^{Arf}$ protein. Again, the $t_{½}$ for $p19^{Arf}$ was ~6 h (Fig. 1B). Studies with MEFs lacking both *p53* and *Mdm2* rendered similar results (Fig. 1C). HA-tagged (Fig. 1A) and endogenous $p19^{Arf}$ proteins (Fig. 1B,C) were degraded at similar rates.

We next introduced a gene encoding p53 fused to a tamoxifen-responsive element of the estrogen receptor (p53ER^{TM}) into *p53*-null MEFs and treated the cells with 4-OH-tamoxifen during the chase period (Fig. 1D). Whereas p53ER^{TM} activation rapidly led to Mdm2 expression, the rate of turnover of endogenous $p19^{Arf}$ was unaffected. Therefore, despite the fact that Arf, Mdm2, and p53 regulate one another's synthesis, neither Mdm2 nor p53 affected the degradation of the endogenous $p19^{Arf}$ protein.

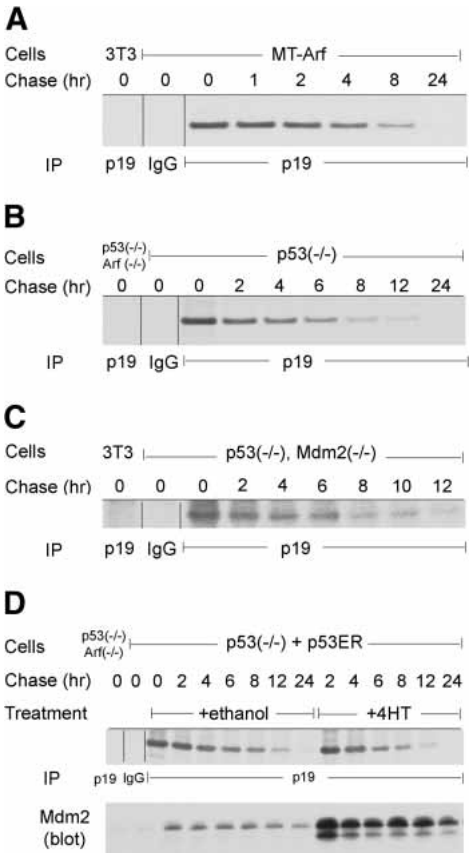

Figure 1. Kinetics of $p19^{Arf}$ turnover. (*A*) MT-Arf cells induced for 10 h with 100 µM $ZnSO_4$ were starved for 30 min in fresh leucine-free medium, metabolically labeled for 2 h with 10 µCi/mL [^{3}H]-leucine, and chased in fresh complete medium for the indicated times. Cell lysates were immunoprecipitated (IP) with antibodies to $p19^{Arf}$ or with control IgG as indicated *below* the panel. Lysates of control *Arf*-null NIH-3T3 cells treated similarly were also precipitated with antibodies to $p19^{Arf}$ (*left* lane). Proteins separated on denaturing gels were transferred to a membrane, treated with EN^{3}HANCE, and subjected to radiofluorography at –80°C using an intensifying screen. (*B*) MEF cultures derived from *p53*-null embryos were starved of leucine, metabolically labeled with 100 µCi/mL [^{3}H]-leucine, and the endogenously expressed Arf protein was analyzed as above. MEFs lacking both *p53* and *Arf* were used as a control (*left* lane). (*C*) MEFs lacking *p53* and *Mdm2* were analyzed identically to those in *B*. (*D*) *p53*-null MEFs engineered to express p53-ER^{TM} were starved and labeled with 100 µCi/mL [^{3}H]-leucine. Cells were chased in fresh medium containing ethanol or 4-hydroxytamoxifen (4HT) as indicated, and lysates were precipitated with antibodies to $p19^{Arf}$ and analyzed (*top* panel). Aliquots of the same lysates were immunoblotted with antibodies to Mdm2 (*bottom* panel), a representative p53-inducible gene.

Hypomorphic Arf mutants are unstable

Mouse *Arf* truncation mutants specified only by exon 1β sequences (Quelle et al. 1997) as well as the natural exon 1β-coded chicken Arf protein (Kim et al. 2003) are fully biologically active. However, a hypomorphic *Arf* mutant lacking residues 2–14 (*Arf* Δ2–14) encodes a defective protein that binds poorly to Mdm2, fails to readily induce p53, and is handicapped in inducing cell-cycle arrest (Weber et al. 1999). This mutant also binds poorly to NPM/B23 and, when overexpressed, is unable to interfere with nucleolar rRNA processing (Sugimoto et al. 2003). Deletion of residues 26–37 reduces Arf's binding affinity for Mdm2 and results in relocalization of much of $p19^{Arf}$ from the nucleolus to the nucleoplasm, whereas deletion of residues 38–52 has no obvious effect (Weber et al. 1999).

Alignment of predicted amino acid sequences encoded by mouse *Arf* exon 1β with those of other species defined six invariant residues (Fig. 2A) that were converted to

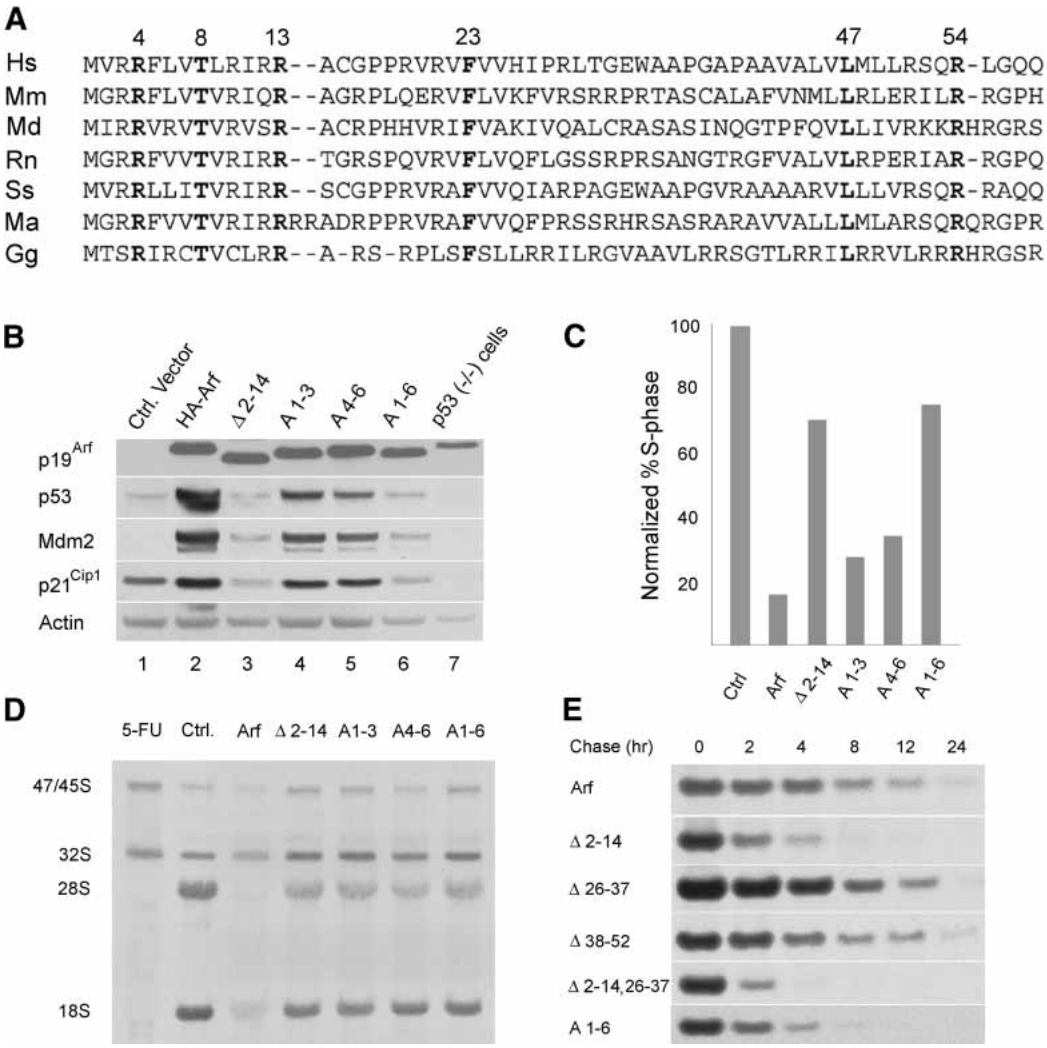

Figure 2. Analysis of Arf mutants. (*A*) N-terminal sequences encoded by *Arf* exon 1β are shown. (Hs) *Homo sapiens*; (Mm) *Mus musculus*; (Md) *Monodelphis domestica*, opossum; (Rn) *Rattus norvegicus*; (Ss) *Sus scrofa*, domestic pig; (Ma) *Mesocricetus auratus*, golden hamster; (Gg) *Gallus gallus*, chicken. (*B*) Lysates of NIH-3T3 cells infected with retroviruses encoding the indicated Arf mutants or an empty vector (Ctrl) were separated on denaturing gels, transferred to membrane, and blotted with antibodies to the indicated proteins. *p53*-null cells (lane 7) that overexpress endogenous $p19^{Arf}$ were used as a control, and antibodies to actin were used to control for protein loading. (*C*) NIH-3T3 cells infected as in *B* were stained with propidium iodide 48 h postinfection and analyzed for DNA content by flow cytometry. The percentage of cells in S phase was determined compared to the S-phase fraction (normalized to 100%) of cells infected with a control vector lacking *Arf*. (*D*) NIH-3T3 cells infected for 48 h with the indicated *Arf* or control retroviral vectors were metabolically labeled for 30 min with 2.5 μCi/mL [^{3}H]-uridine and reincubated in fresh medium for 2 h. Where indicated, cells were exposed to 5 μM 5-fluorouridine (5-FU) 15 min prior to metabolic labeling to prevent rRNA processing. Extracted RNAs were separated on 1% agarose gels, transferred to a Hybond N+ membrane, treated with EN^{3}HANCE, and subjected to autofluororadiography at −80°C using an intensifying screen. The positions of 47/45S and 32S rRNA precursors and mature 28S and 18S rRNAs are indicated. (*E*) NIH-3T3 cells infected with retroviral vectors encoding the indicated *Arf* mutants were subjected to pulse-chase analysis 48 h postinfection as in Figure 1A.

alanines. Mutant A1–3 contains Ala replacements at Arg 4, Thr 8, and Arg 13; A4–6 has Ala substitutions for Phe 23, Leu 47, and Arg 54; and A1–6 contains alanine at all six positions. Like wild-type $p19^{Arf}$ and $p19^{Arf}$ Δ2–14, transduced substitution mutants localized to nucleoli (Supplementary Fig. 1). When highly expressed, Arf Δ2–14 and Arf A1–6 were handicapped in inducing p53 or the p53-responsive gene products, Mdm2 and $p21^{Cip1}$ (Fig. 2B) and in arresting the cell cycle (Fig. 2C). Moreover, like Arf Δ2–14, none of the substitution mutants efficiently retarded rRNA processing (Fig. 2D).

Arf Δ2–14 and Arf A1–6 were markedly unstable, exhibiting half-lives of ~2 h (Fig. 2E). In contrast, two other *Arf* exon-1β deletion mutants, Arf Δ26–37 (lacking none of the six most conserved residues) and Arf Δ38–52 (lacking Leu 47), were degraded at rates like that of the wild-type protein. The Arf A1–3 and Arf A4–6 proteins exhibited intermediate turnover rates of ~4 h (data not shown).

Thus, the impaired biologic functions of these Arf mutants correlated with their reduced stability.

p19^{Arf} is degraded in the proteasome

After induction of MT-Arf cells with submaximal concentrations of zinc, treatment of cells with MG132, a proteasome inhibitor, led to increased p19^{Arf} accumulation (Fig. 3A). The levels of p53 and p21^{Cip1}, two proteins whose turnover is proteasome-dependent, were also increased by MG132 treatment, irrespective of whether p19^{Arf} was induced (Fig. 3A). When added during the chase period, MG132 extended the half-life of p19^{Arf} from 6 to >10 h (Fig. 3B). MT-Arf cells withdrew from the cell cycle within 24 h of zinc treatment, but in the presence of MG132, they began to die. However, Arf induction or MG132 treatment alone had no such effects on cell viability, so initiation of an apoptotic program could have limited the MG132-induced stabilization of both p19^{Arf} and p21^{Cip1} after 24 h of chase (Fig. 3B).

MG132 had even more marked effects in facilitating the accumulation of labile Arf mutants. NIH-3T3 cells infected with retroviruses encoding Arf Δ2–14 or the three Arf alanine substitution mutants accumulated much higher levels of the mutant polypeptides in cells treated with MG132 versus DMSO (Fig. 3C). E64, an inhibitor of cysteine proteases that does not affect the proteasome, had no such effect (Fig. 3C). The t½ of p19^{Arf} Δ2–14 was prolonged following MG132 treatment (Fig. 3D) although to a much lesser extent than that of full-length p19^{Arf} (Fig. 3B). Thus, wild-type p19^{Arf} and the less stable Arf variants are all stabilized by the proteasome inhibitor, but degradation of unstable Arf mutants still proceeded more rapidly than that of wild-type p19^{Arf}. Possibly, MG132 is not fully effective in blocking degradation of highly unstable proteins or, conceivably, these Arf mutants may also be subject to degradation via a nonproteasomal pathway.

p19^{Arf} turnover depends on the ubiquitin-activating E1 enzyme

We next introduced HA-tagged Arf proteins into tsBN75 cells that express a temperature-sensitive (ts) ubiquitin-activating E1 enzyme (Nishimoto et al. 1980). Cells were maintained at the permissive temperature of 34°C or were shifted to the nonpermissive temperature of 40°C, after which Arf protein levels were determined. The wild-type p19^{Arf} protein and Arf A1–3 accumulated at 40°C, but Arf Δ2–14 and Arf A1–6 seemingly did not (Fig. 4A). Mutant A4–6 exhibited an intermediate response to E1 enzyme depletion. As expected, p53 accumulated at 40°C irrespective of Arf expression (Fig. 4A).

Increased temperature per se might accelerate the turnover of Arf proteins, leading at 40°C to a more rapid degradation of the already destabilized Arf Δ2–14 and Arf A1–6 mutants and countering effects of E1 inactivation. When the vectors were introduced into NIH-3T3 cells grown at both 34°C and 40°C, wild-type p19^{Arf} and Arf mutants Δ2–14 and A1–6 accumulated to lower levels at the elevated temperature, indicating that the stability of all three proteins is highly temperature-dependent (Fig. 4B). Given these findings, we repeated temperature shift

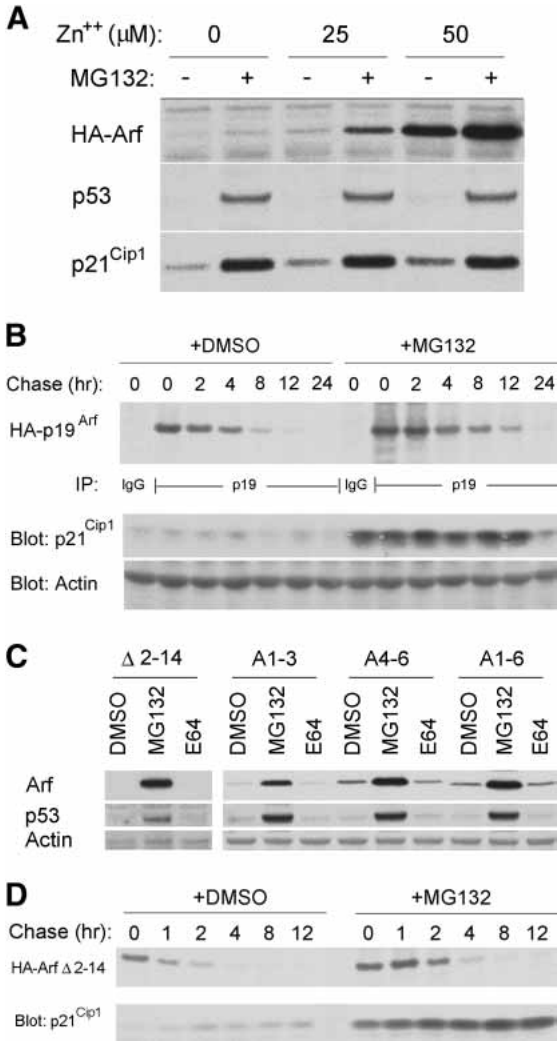

Figure 3. Stabilization of Arf by proteasome inhibition. (*A*) MT-Arf cells induced for 10 h with the indicated concentrations of $ZnSO_4$ were cultured in fresh medium containing DMSO or 10 μM MG132 for an additional 8 h. Proteins from cell lysates were separated on a denaturing gel and blotted with antibodies to the indicated proteins. (*B*) Kinetic analysis of p19^{Arf} turnover was performed as in Figure 1A, except that MT-Arf cells were induced with 50 μM $ZnSO_4$, after which DMSO or MG132 was added to the labeling and chase medium. Proteins were blotted with antibodies to p21^{Cip1}, which accumulates in response to MG132. Actin was used to control for protein loading. (*C*) NIH-3T3 cells infected for 48 h with retroviral vectors encoding the indicated Arf mutants were treated for an additional 24 h with DMSO, MG132, or E64 prior to lysis, electrophoresis, and immunoblotting with antibodies to the indicated proteins. Actin was used as a loading control. (*D*) Pulse-chase analysis was performed as in *B* using NIH-3T3 cells infected with a retroviral vector encoding HA-tagged Arf Δ2–14. Cell lysates were blotted with antibodies to p21^{Cip1} to demonstrate stabilization by MG132.

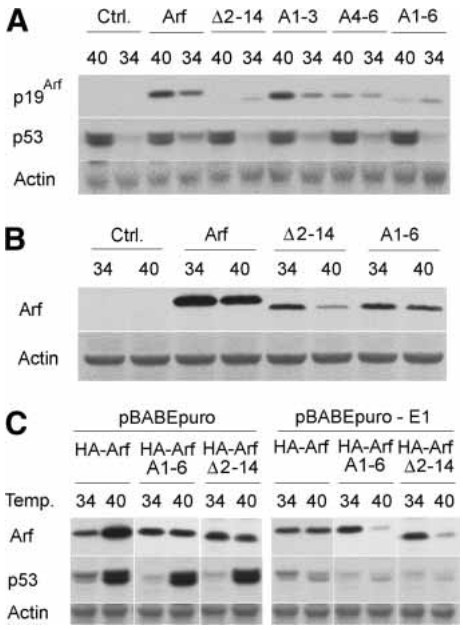

Figure 4. Turnover of Arf proteins in cells expressing temperature-sensitive E1 ubiquitin-activating enzyme. (*A*) Hamster tsBN75 cells infected for 24 h with retroviruses packaged with VSV G protein and encoding the indicated Arf proteins were shifted to 34°C or 40°C for an additional 24 h. Cell lysates were separated on gels and blotted with antibodies to the indicated proteins. (*B*) NIH-3T3 cells infected with retroviral vectors encoding p19^{Arf} and the indicated mutants were analyzed as in *A*. (*C*) tsBN75 cells were infected with pBABEpuro retroviral vectors (packaged in VSV G protein) either lacking or containing the gene encoding the E1 ubiquitin-activating enzyme. After selection for 48 h in puromycin, surviving cells were expanded and reinfected with VSV G protein-packaged vectors encoding the indicated Arf proteins. Twenty-four hours postinfection, cells were shifted to 34°C or 40°C for an additional 24 h. Cell lysates were separated, transferred to membrane, and blotted with antibodies to the indicated proteins. Actin was used as a loading control in each experiment.

experiments in tsBN75 cells infected with a control vector or one encoding wild-type E1 (Fig. 4C). Accumulation of HA-tagged wild-type p19^{Arf} at 40°C was abrogated by E1 re-expression. Although the HA-Arf A1–6 and Δ2–14 mutants failed to accumulate at 40°C in cells infected with the control vector, the levels of both proteins were significantly reduced in cells re-expressing E1 (Fig. 4C), clearly demonstrating their dependency on the ubiquitin-activating enzyme. Thermal inactivation of a subunit of the E1 enzyme (APP-BP1) for the ubiquitin-like protein NEDD8 had no effect on Arf turnover, apart from the labilization of Arf proteins by heat shock (Supplementary Fig. 2). Thus, p19^{Arf} turnover specifically depends on the ubiquitin-conjugating machinery.

p19^{Arf} is polyubiquitinated

To test whether p19^{Arf} itself undergoes ubiquitination, we expressed untagged p19^{Arf} in 293T cells together with a second vector encoding HA-ubiquitin. Transfected 293T cells were either left untreated or were treated with MG132. When p19^{Arf} was recovered with cognate antibodies and blotted with antibodies to HA, we detected a ladder of HA-marked molecules (Fig. 5A, lane 4) whose intensity was increased after MG132 treatment (Fig. 5A, lane 5). In turn, when the same samples were blotted with antibodies to p19^{Arf} itself, overexposure of the film demonstrated a similar ladder of Arf species (Fig. 5A, lanes 9,10). As expected, p19^{Arf} itself could not be detected with antibodies to HA (Fig. 5A, lanes 3–5). Importantly, the fastest migrating species in lanes 4 and 5 in Figure 5A corresponded in molecular mass to that predicted for mono-HA-ubiquitinated p19^{Arf} (Fig. 5A, lanes

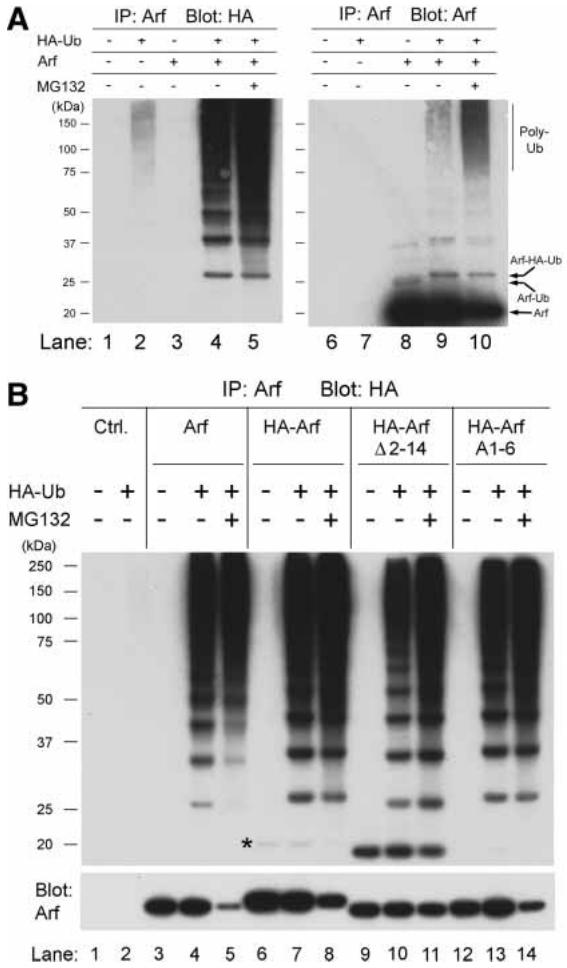

Figure 5. Mouse p19^{Arf} is polyubiquitinated. (*A*) Human 293T cells were cotransfected with vectors encoding HA-tagged ubiquitin and/or p19^{Arf} and, 24 h posttransfection, were either left untreated or were treated for 16 h with MG132. Lysates were immunoprecipitated (IP) with antibodies to p19^{Arf}, and separated proteins were blotted with antibodies to the HA-tag (*left*) or to p19^{Arf} (*right*). The mobilities of p19^{Arf}, mono-ubiquitinated p19^{Arf} (Arf-Ub), mono-HA-ubiquitinated p19^{Arf} (Arf-HA-Ub), and polyubiquitinated forms (poly-Ub) are indicated at the far *right*. (*B*) Experiments analogous to those in *A* were performed using the indicated untagged or HA-tagged Arf proteins. The asterisk designates un-ubiquitinated HA-Arf.

9,10). A slightly faster migrating form of Arf was detected in cells that had not been transfected with HA-ubiquitin (Fig. 5A, lane 8). This species was not detected with antibodies to HA (Fig. 5A, lane 3), suggesting that it represented a modified form of Arf containing endogenous untagged mono-ubiquitin. We obtained similar results using modified versions of Arf that contained either one or three tandem Flag tags at their N and C termini, respectively, providing further evidence that Arf itself, and not simply other coprecipitating proteins underwent ubiquitination (Supplementary Fig. 3). A caveat, however, is that unlike the HA tag, the Flag tag contains lysine residues.

Because turnover of unstable Arf mutants also depended upon the ubiquitin-conjugating system, we compared ubiquitination of wild-type $p19^{Arf}$ with that of HA-Arf Δ2–14 and HA-Arf A1–6. Cells transfected with vectors encoding untagged wild-type Arf, HA-Arf, HA-Arf Δ2–14, and HA-Arf A1–6, were either cotransfected with the vector encoding HA-ubiquitin or not, and some cotransfected cultures were treated with MG132. Cell lysates were precipitated with antibodies to $p19^{Arf}$, and separated proteins were blotted with anti-HA (Fig. 5B). Cells infected with an empty control vector (Fig. 5B, lane 1) or with vectors encoding either HA-ubiquitin (Fig. 5B, lane 2) or untagged-Arf alone (Fig. 5B, lane 3) yielded no HA signal. In contrast, cells cotransfected with vectors encoding HA-ubiquitin and Arf proteins yielded ladders of mono-HA- and poly-HA-ubiquitinated proteins. Untagged $p19^{Arf}$ underwent ubiquitination (Fig. 5B, lane 4), and more polyubiquitinated forms accumulated in the presence of MG132 (Fig. 5B, lane 5) with a concomitant drop in the level of nonubiquitinated $p19^{Arf}$ (Fig. 5B, Arf blot, bottom, lane 5). Antibodies to HA detected the nonubiquitinated HA-Arf protein (Fig. 5B, lane 6, designated with asterisk) as well as ladders of mono-HA and polyubiquitinated forms (Fig. 5B, lanes 7,8) whose mobilities were slower than those generated with untagged $p19^{Arf}$ (Fig. 5B, cf. lanes 7 and 4 and lanes 8 and 5). Conversely, HA-Arf Δ2–14 migrated faster than full-length HA-Arf (Fig. 5B, cf. lanes 9 and 6), as did its ubiquitinated derivatives (Fig. 5B, cf. lanes 10,11 and 7,8). The antibodies to HA more readily detect Arf Δ2–14 (Fig. 5B, cf. lanes 9–11 and 6–8), probably reflecting greater accessibility to the N-terminal epitope. HA-Arf A1–6 was also ubiquitinated (Fig. 5B, lanes 12–14). The remarkably steady spacing of these ubiquitin ladders strongly suggested that a single polyubiquitin chain of variable length was attached to only one site within the various Arf proteins.

Arf is ubiquitinated at its N terminus

Mouse $p19^{Arf}$ contains only a single lysine (Lys 26) that is not conserved in human $p14^{ARF}$ or in Arf proteins of most other species (Fig. 2A). Introduction of the human lysine-less *ARF* gene into tsBN75 cells demonstrated that human $p14^{ARF}$, like its murine counterpart, was stabilized after E1 inactivation (Fig. 6A). Moreover, cotransfection experiments identical to those shown in Figure 5B indicated that human $p14^{ARF}$ and a $p14^{ARF}$ Δ2–14 mutant were ubiquitinated (Fig. 6B), and that the $p14^{ARF}$ Δ2–14 mutant was also highly unstable (Fig. 6E, top panel). Similar results were obtained with a mouse Arf mutant in which Lys 26 was mutated to an arginyl residue (K26R). Not only was HA-tagged, $p19^{Arf}$ K26R stabilized at 40°C in tsBN75 cells (Fig. 6C) but it was polyubiquitinated when cotransfected with HA-ubiquitin into 293T cells (Fig. 6D). Moreover, the turnover rate of HA-Arf K26R was virtually identical to that of the parent molecule (Fig. 6E, bottom). We therefore explored the possibility that Arf might undergo N-terminal ubiquitination.

Based on a strategy employed by Bloom et al. (2003), we inserted a factor Xa protease cleavage site between the HA-leader and the body of the Arf Δ2–14 protein. We used this mutant because it fails to efficiently bind to both Mdm2 (Weber et al. 1999) and NPM/B23 (Bertwistle et al. 2004), but is polyubiquitinated (Fig. 5B). Importantly, we maintained the Arf N-terminal dipeptide sequence (Met–Gly) upstream of the HA-tag to avoid N-terminal acetylation (see below). After coexpression of Arf with His-ubiquitin in 293T cells, lysates were either treated with Xa protease or not, and His-tagged proteins recovered on nickel columns in the presence of 8 M urea were separated on denaturing gels and blotted with antibodies to HA. Because unconjugated His-ubiquitin was present in excess, detection of ubiquitin-modified proteins required long exposures of the blots. Under these conditions we detected nonspecific binding of unmodified HA-Arf Δ2–14 to the affinity resin (Fig. 7A, lane 3, arrow), which was increased when other His-ubiquitinated proteins were also bound (Fig. 7A, lanes 5,6). Pretreatment of lysates with factor Xa protease prior to chromatography released most of the HA-tag from HA-Arf Δ2–14 (Fig. 7A, cf. lanes 4 and 3 and lanes 6 and 5). Without prior protease treatment, we recovered poly-His-ubiquitinated HA-Arf species (Fig. 7A, lane 5, asterisks). In contrast, Xa protease cleavage liberated the HA-tagged N-terminal segment, so that more rapidly migrating His-ubiquitin HA-tagged chains were recovered at the expense of polyubiquitinated Arf species (Fig. 7A, lane 6, asterisks). Longer exposures (Fig. 7A, lanes 7,8) corresponding to lanes 5 and 6 in Figure 7A also identified HA-tagged His-ubiquitin chains unbound to Arf (Fig. 7A, lane 8, asterisks). Identical results were obtained with a construct containing the K26R substitution (data not shown). Not only did these results indicate that Arf is ubiquitinated at its N terminus, but they also implied that ubiquitination did not occur at K26.

In order for untagged or HA-tagged $p19^{Arf}$ to undergo N-terminal ubiquitination, its N-terminal amino group must be unblocked. The N-terminal methionine of $p19^{Arf}$ (NH_2-Met–Gly–Arg), $p14^{ARF}$ (NH_2-Met–Val–Arg), and the HA-tag used in our studies (NH_2-Met–Gly–Tyr) should each be cleaved by methionine aminopeptidase (Bradshaw et al. 1998) generating sequence motifs that are predicted to be very poor substrates for N-terminal acetyltransferases (Polevoda and Sherman 2003). Based on these considerations, we constructed lysine-less Arf mutants whose N termini are acetylated (Supplementary

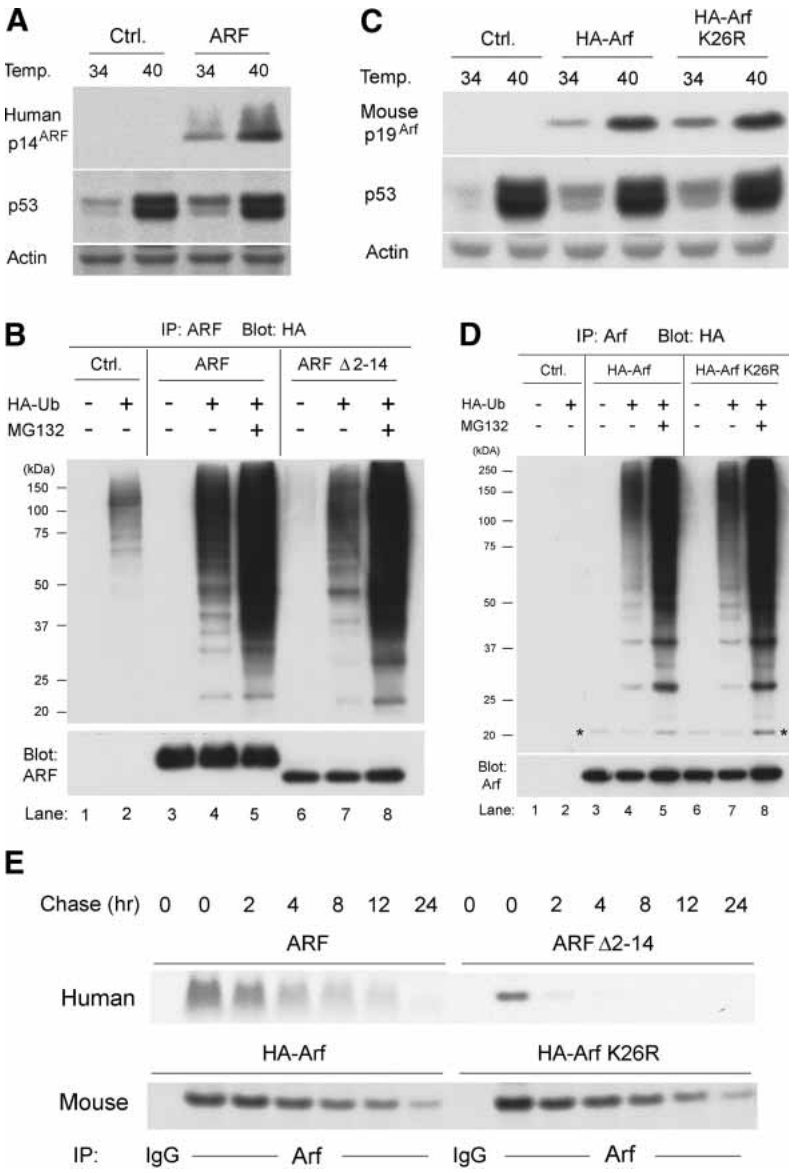

Figure 6. E1 dependency and ubiquitination of human p14^{ARF} and mouse lysine-less p19$^{Arf.}$ (*A*) ts-BN75 cells containing a thermolabile E1 enzyme were infected with a VSV G protein-packaged retroviral vector encoding untagged human p14^{ARF}. Twenty-four hours postinfection, cells were shifted to 34°C or 40°C for an additional 24 h. Proteins separated on denaturing gels were transferred to membrane and blotted with antibodies to proteins indicated at the *left*. Actin was used as a loading control. (*B*) Human 293T cells transfected with retroviral expression vectors encoding untagged human p14^{ARF}, human ARF Δ2–14, and/or HA-tagged ubiquitin (HA-Ub) were either left untreated or exposed to MG132. Equal amounts of lysate protein were precipitated with antibodies to human p14^{ARF}, and separated proteins were blotted with antibodies to HA (*top* panel) or to p14^{ARF} (*bottom* panel). (*C*) ts-BN75 cells infected with vectors encoding HA-tagged mouse p19^{Arf} or a lysine-less mutant (K26R) were analyzed as in *A*. (*D*) Human 293T cells transfected with retroviral expression vectors encoding HA-tagged mouse p19^{Arf} or the lysine-less K26R mutant were analyzed as in *B*. The asterisks in the *upper* panel indicate the position of the unubiquitinated HA-Arf proteins. (*E*) Pulse-chase analyses of human p14^{ARF} and p14^{ARF} Δ2–14 (*top* panel) and mouse HA-p19^{Arf} and the K26R mutant (*bottom* panel) expressed in NIH-3T3 cells.

Fig. 4). These were expressed in 293T cells together with His-tagged ubiquitin, and ubiquitinated proteins again recovered on nickel columns were separated and blotted with a monoclonal antibody to p19^{Arf}. The mutant Arf proteins were not as efficiently ubiquitinated (Fig. 7B), and their half-lives were extended by ~2 h (Fig. 7C). Similar results were obtained with human p14^{ARF} (data not shown). Therefore, the Arf N-terminal amino acid sequence determines its ubiquitination and turnover.

NPM/B23 stabilizes Arf

The vast majority of p19^{Arf} localizes to high-molecular-weight complexes that contain NPM/B23 (Itahana et al. 2003; Bertwistle et al. 2004), and such interactions might affect Arf degradation. Two naturally occurring NPM/B23 isoforms arise by alternative splicing. Full-length NPM (B23.1) contains a nucleic acid binding domain at its C terminus that is absent from B23.2; a similar mutant (ΔC1) was constructed by C-terminal truncation of the full-length NPM/B23 molecule. Both forms of NPM/B23 bind strongly to Arf. However, overexpression of the ΔC1 mutant relocalizes Arf from 2- to 5-Mda complexes to smaller complexes of ~500 kDa and interferes with Arf's ability to retard rRNA processing (Bertwistle et al. 2004).

We therefore infected MT-Arf cells with retroviruses encoding the two N-terminally Flag-tagged versions of NPM/B23. Although NPM/B23.1 is a relatively abundant protein, retroviral infection resulted in an approximately twofold increase in its level. In contrast, MT-Arf cells make little B23.2. We treated cells overexpressing NPM/B23 with zinc to induce Arf and then performed pulse-chase analyses (Fig. 8A). The t½ of p19^{Arf} in cells

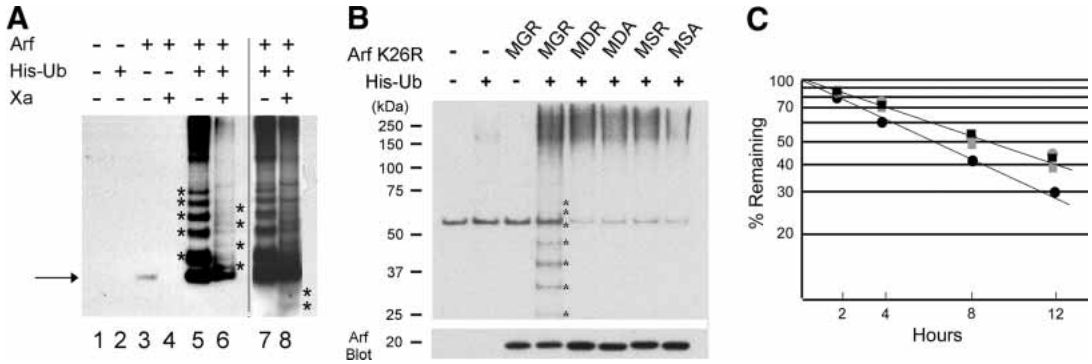

Figure 7. N-terminal sequences determine Arf ubiquitination and turnover. (*A*) Human 293T cells transfected with HA-Arf Δ2–14 containing a factor Xa cleavage site C-terminal to the HA tag and/or His-ubiquitin were lysed and treated with protease Xa or not (indicated at *top*). Proteins recovered on nickel affinity columns in the presence of 8 M urea were separated on gels and blotted with anti-HA. The position of unmodified Arf protein is indicated by the arrow (*left*) and ubiquitinated species by asterisks. (Lanes *7*,*8*) Longer exposures of lanes *5* and *6* reveal cleaved HA-tagged His-ubiquitin chains unbound to Arf. (*B*) 293T cells transfected with vectors encoding the indicated Arf N-terminal mutants and His-tagged ubiquitin were recovered, separated, and blotted with antibody to $p19^{Arf}$. A background band at ~55 kDa was detected in all lanes. Asterisks denote the lower-molecular-weight ubiquitinated Arf species. (*Bottom*) Immunoblotting was used to estimate the amounts of Arf protein loaded in each lane. (*C*) NIH-3T3 cells were infected with retroviral vectors encoding wild-type $p19^{Arf}$ and Arf variants engineered to undergo less efficient N-terminal ubiquitination. Pulse-chase analysis was used to compare the half-life of wild-type $p19^{Arf}$ (MGR, black circles) with the N-terminal mutants. (Gray circles) MDR; (black squares) MSA; (gray squares) MSR.

infected with a control vector was ~6 h, whereas its stability was greatly increased ($t_{½}$ ~ 12 h) in cells enforced to overexpress Flag-tagged NPM/B23 (Fig. 8A). The ΔC1 mutant was somewhat more effective than full-length NPM/B23 in inhibiting $p19^{Arf}$ turnover. In turn, MT-Arf cells were infected with retroviral vectors encoding interfering short hairpin (sh)RNAs to NPM/B23, and following puromycin selection for 48 h, the cells were induced with zinc, and the levels of NPM/B23 and $p19^{Arf}$ were determined by immunoblotting after zinc removal. Introduction of three different shRNAs each lowered the level of NPM/B23 by ~50%, and this accelerated Arf degradation (Fig. 8B).

To determine whether NPM/B23 would bind to unstable Arf mutants, these were introduced into 293T cells. Immunoprecipitates of endogenous NPM/B23 prepared from equal quantities of detergent-solubilized cellular proteins were separated on denaturing gels and blotted with antibodies to Arf (Fig. 8C, top panels). Although very similar amounts of NPM were precipitated from each of the infected cell lines, the amounts of coprecipitating Arf Δ2–14 and Arf A1–6 were significantly lower than those recovered from cells expressing wild-type Arf. Arf mutants A1–3 and A4–6 were far less impaired in their ability to associate with NPM/B23. Using equivalent amounts of the same cell lysates, we recovered the Arf proteins and evaluated the levels of coprecipitating NPM/B23 (Fig. 8C, bottom). Similar levels of Arf were recovered from the different cell lines, but significantly less NPM/B23 was coprecipitated from cells expressing mutant forms of Arf. Again, Arf Δ2–14 and Arf A1–6 were the most impaired in associating with NPM/B23. Therefore, Arf is stabilized through its association with NPM/B23, but those Arf mutants that fail to strongly interact with NPM/B23 are more rapidly degraded. Enforced coexpression of NPM/B23 or the ΔC1 mutant together with $p19^{Arf}$ and HA-ubiquitin in 293T cells did not appreciably inhibit Arf polyubiquitination (Supplementary Fig. 5), suggesting that the interaction of Arf with NPM/B23 does not block the Arf N terminus.

Discussion

Mouse $p19^{Arf}$ turns over with a half-life of ~6 h, but degradation of two mutants, Arf Δ2–14 and Arf A1–6, was greatly accelerated. These mutant proteins did not effectively bind to either Mdm2 or NPM/B23 and were impaired in their ability to arrest the cell cycle or inhibit rRNA processing, suggesting that they may be improperly folded and more readily recognized by the cell's protein degradation machinery. Studies with MG132 indicated that $p19^{Arf}$ and all variants studied thus far are degraded, at least in part, by the proteasome. Although most cellular proteins degraded in the proteasome are ubiquitinated, proteins such as ornithine decarboxylase (Li and Coffino 1992), tau (David et al. 2002), and the Cdk inhibitor $p21^{Cip1}$ (Sheaff et al. 2000) can be directed to the proteasome without prior ubiquitination. Even for those proteins that require ubiquitination for their proteasomal recognition and destruction, their rate of degradation can be enhanced by the presence of loosely structured peptide segments that facilitate rapid unfolding by proteasomal ATPases (Verma and Deshaies 2000), and the proximity of such misfolded segments to sites of ubiquitination may be important in determining their turnover rates (Petroski and Deshaies 2003). Therefore, we wished to determine whether $p19^{Arf}$ underwent ubiquitination and, if so, to elucidate whether this process determined its half-life in vivo.

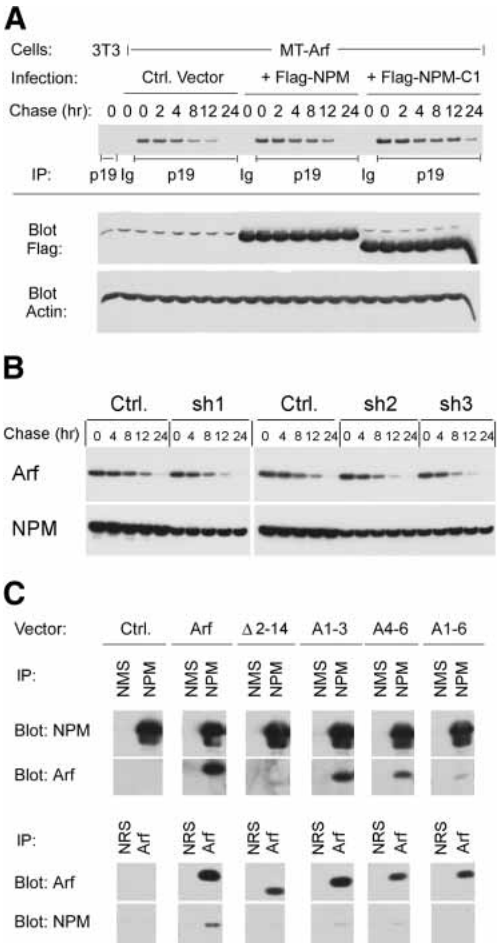

Figure 8. Stabilization of $p19^{Arf}$ by NPM/B23. (*A*) MT-Arf variants were derived by infection with a control retroviral vector expressing GFP or with vectors expressing Flag-tagged full-length NPM or a truncated mutant (ΔC1) lacking the C-terminal RNA-binding domain. Cells induced for 10 h with 100 µM $ZnSO_4$ were incubated in fresh leucine-free medium for 30 min, labeled with [^{3}H]-leucine for 2 h, and chased with complete medium for the indicated times. (*Top*) Cell lysates were immunoprecipitated (IP) with antibodies to $p19^{Arf}$, and separated proteins were transferred to a membrane and detected by fluororadiography. (*Bottom*) Samples of the same cell lysates were separated and blotted with antibodies to the Flag-tag or to actin as a loading control. (*B*) MT-Arf cells infected with retroviruses encoding three different shRNAs to NPM/B23 were induced with 50 µM zinc for 10 h, after which zinc was removed. Cell lysates prepared at the indicated times thereafter (chase) were blotted with antibodies to $p19^{Arf}$ or NPM/B23. (*C*) 293T cells transfected with retroviral vectors encoding the indicated Arf proteins were lysed, and proteins (500 µg aliquots) were immunoprecipitated (IP) with normal mouse serum (NMS), normal rabbit serum (NRS), or antibodies to NPM or $p19^{Arf}$. (*Left*) Separated proteins were transferred to a membrane and blotted with antibodies to NPM or Arf as indicated.

Arf turnover depends on the ubiquitin-conjugating system

Cells bearing a ts-E1 ubiquitin-activating enzyme are defective in ubiquitin conjugation at the nonpermissive temperature. These cells accumulated $p19^{Arf}$ at 40°C, indicating that $p19^{Arf}$ turnover depends, at least in part, upon the ubiquitin–proteasome pathway. Reintroduction of the wild-type E1 enzyme into tsBN75 cells propagated at the nonpermissive temperature reversed this process. In contrast, another temperature-sensitive E1 enzyme that is important for a different ubiquitin-like modification, neddylation, had no effect on $p19^{Arf}$ turnover.

The rate of $p19^{Arf}$ turnover is itself temperature-dependent, so that degradation of the less stable Arf mutants initially appeared not to depend on the E1 ubiquitin-conjugating enzyme. However, by reintroducing the E1 enzyme into tsBN75 cells grown at the nonpermissive temperature, we demonstrated that the ubiquitination pathway played a role in the degradation of Arf Δ2–14 and Arf A1–6 as well. Similar results were obtained with lysine-less human $p14^{ARF}$ and the mouse K26R Arf mutant.

Arf proteins are ubiquitinated, but lysines are not required

$p19^{Arf}$ could be covalently modified by HA-ubiquitin, whether Arf was expressed in its native form or was tagged with a lysine-less HA epitope inserted just downstream of the Arf Met–Gly N terminus. Importantly, immunoblotting with an antibody to Arf revealed higher-molecular-weight, HA-ubiquitin-tagged forms of $p19^{Arf}$ itself. A potentially confounding finding is that human $p14^{ARF}$ aggregates under oxidizing conditions, even in denaturing gels (Menendez et al. 2003), but in cells that did not coexpress HA-ubiquitin, we did not see significant accumulation of high-molecular-weight forms of mouse $p19^{Arf}$ under reducing conditions. It is also quite conceivable that the poly-HA-ubiquitinated proteins detected in some of our experiments might have included other proteins such as NPM/B23, which coprecipitates with $p19^{Arf}$ (Bertwistle et al. 2004) and also undergoes ubiquitination (Itahana et al. 2003). To avoid this complication, cells were lysed in buffers containing multiple detergents, including SDS, in which Arf's association with NPM and other proteins is minimized. Under these conditions, the electrophoretic mobilities of the presumptively mono-HA-ubiquitinated Arf species on denaturing gels consistently corresponded to those predicted from the molecular masses of untagged or differentially tagged forms of the protein. Similarly, when $p19^{Arf}$ was coexpressed with His-tagged ubiquitin and ubiquitinated proteins were recovered in 8 M urea, immunoblotting with antibodies to Arf again revealed slower-migrating, laddered forms of the protein. Thus, $p19^{Arf}$ itself, and not just coprecipitating proteins, contained ubiquitin.

Lysine-less human ARF and the mouse Arf K26R mutant were ubiquitinated as efficiently as lysine-containing wild-type $p19^{Arf}$ and were degraded at similar rates. As for untagged or HA-tagged $p19^{Arf}$, the mobilities of mono-HA-ubiquitinated $p14^{ARF}$ and $p19^{Arf}$ K26R corresponded to their predicted molecular masses on denaturing gels. Ladders of polyubiquitinated species were

readily formed, and these were further stabilized by proteasome inhibition. Importantly, the steady spacing of HA- or His-ubiquitinated $p19^{Arf}$ species observed in these experiments strongly suggested that one polyubiquitin chain of variable length was attached to a single site within these lysine-less proteins.

We considered the possibility that some Arf protein might misincorporate lysine for arginine during translation, thereby enabling the resulting Arf variants to be ubiquitinated. However, despite the fact that Arf contains ~22% arginyl residues, the different arginyl tRNAs in mammalian cells are relatively abundant, and in studies utilizing protamine, the misincorporation rate of lysine for arginine in cell-free reticulocyte translation systems is very low (0.06%–0.2%; Mori et al. 1985). Cell-free translation of $p19^{Arf}$ K26R failed to demonstrate misincorporation of lysine (data not shown), although, arguably, the method may not be sufficiently sensitive to detect random inclusion of lysine residues into few molecules. In principle, ubiquitin can also be attached to serine, threonine, and cysteine residues by ester bonds, but such conjugates have never been demonstrated, and they would not withstand the boiling conditions used in preparing proteins for separation in SDS-containing gels (Breitschopf et al. 1998).

Arf is ubiquitinated at its N terminus

By introducing a protease cleavage site downstream of the HA-tag, we were able to demonstrate that polyubiquitin was conjugated to the $p19^{Arf}$ N terminus, but seemingly not to Lys 26. These data are consistent with observations that $p19^{Arf}$ and the lysine-less K26R Arf mutant were degraded at similar rates. Nonetheless, the features that determine the specificity of ubiquitination on different amino groups remain unclear. For example, although the yeast cyclin-dependent kinase (Cdk) inhibitor, Sic1, is normally ubiquitinated at multiple internal lysines, ubiquitination at a single lysyl residue is sufficient to guarantee Sic1 targeting to, and degradation by, proteasomes at physiologic rates (Petroski and Deshaies 2003). However, reinsertion of single lysyl residues at various positions within lysine-less Sic1 yielded mutant proteins with widely different half-lives.

From a purely chemical perspective, the ubiquitin transfer reaction simply requires a free primary amino group, but only a few proteins have been found to be polyubiquitinated at their N termini (Breitschopf et al. 1998; Aviel et al. 2000; Reinstein et al. 2000; Bloom et al. 2003; Ciechanover and Ben-Saadon 2004). One explanation is that the vast majority of proteins in eukaryotic cells undergo N-terminal acetylation (Polevoda and Sherman 2003). Cleavage of N-terminal methionine is dictated by the adjacent amino acid, so that the seven amino acids with the smallest radii of gyration are processed by methionine aminopeptidases (Bradshaw et al. 1998). N-terminal serine, alanine, and unprocessed methionine are routinely acetylated, whereas glycine and valine are poor acceptors. The penultimate residue profoundly affects the efficiency of acetylation, with acidic residues promoting acetylation and basic ones inhibiting it. Notably, $p19^{Arf}$ (Met–Gly–Arg), $p14^{ARF}$ (Met–Val–Arg), and our HA-tagged $p19^{Arf}$ construct (Met–Gly–Tyr) should be efficiently processed by methionine aminopeptidase but not acetylated, thereby allowing ubiquitination to proceed. Arf mutants containing better consensus sites for N-terminal acetylation were stabilized, providing evidence that N-terminal polyubiquitination can limit Arf's half-life.

To date, all examples of N-terminal ubiquitination have involved mutant proteins from which lysyl residues were removed by mutation, and the physiologic significance of N-terminal ubiquitination has remained unclear. A lysine-less mutant of the MyoD transcription factor was polyubiquitinated and degraded by the proteasome in vitro, but chemically N-terminally modified forms were stabilized, whether or not the protein contained internal lysine residues (Breitschopf et al. 1998). A lysine-less mutant of $p21^{Cip1}$ [p21(K0)] turns over nearly as rapidly as its wild-type counterpart (Sheaff et al. 2000), and unmodified $p21^{Cip1}$, which is disordered unless complexed to other proteins (Kriwacki et al. 1996), can be degraded by the 26S proteasome in vitro in the absence of ubiquitination (Liu et al. 2003). However, the p21 (K0) mutant can undergo N-terminal ubiquitination, and competitive overexpression of lysine-less ubiquitin stabilized the p21(K0) protein (Bloom et al. 2003). N-terminal ubiquitination of wild-type $p21^{Cip1}$ is surprising, since its N-terminal sequence (Met–Ser–Glu) should be efficiently processed and acetylated (Bradshaw et al. 1998; Polevoda and Sherman 2003). N-terminal ubiquitination and acetylation might occur competitively (Bloom and Pagano 2004), and in our hands, lysine-less $p19^{Arf}$ mutants engineered to be more efficiently acetylated, while stabilized, still underwent polyubiquitination to a lesser extent.

One degradation pathway or more?

Arf degradation does not depend on either Mdm2 or p53, despite the fact that Mdm2 is an E3 ubiquitin protein ligase with which Arf physically interacts. Notably, the rate of $p19^{Arf}$ turnover was similar in cells undergoing p53-dependent cell-cycle arrest and in *p53*-null cells that remained in cycle. Instead, the stability of $p19^{Arf}$ was significantly increased in cells enforced to overexpress NPM/B23, a protein that binds to $p19^{Arf}$ with much higher stoichiometry than does Mdm2 (Bertwistle et al. 2004). Inhibition of NPM/B23 synthesis with shRNAs destabilized $p19^{Arf}$, and Arf mutants that did not strongly interact with NPM were unstable. NPM-mediated sequestration of $p19^{Arf}$ in high-molecular-weight complexes within the nucleolus might protect it from being accessed by the cell's degradation machinery. Perhaps like "free" $p21^{Cip1}$ (Kriwacki et al. 1996), $p19^{Arf}$ is unstructured unless bound and stabilized in higher-order complexes. Hence, ubiquitination may be a necessary prerequisite in destabilizing Arf proteins in complexes with NPM/B23, but Arf mutants that cannot interact with NPM/B23 might be misfolded in such a way as to

be directly degraded by the proteasome or, conceivably, also via another pathway. Assuming that at least one role of polyubiquitination is to unfold proteins to enable their proteasomal degradation, it is not surprising that ubiquitination, heat shock, and particular mutations in the protein itself can each contribute to destabilizing $p19^{Arf}$ and promoting its degradation. A deeper understanding of these processes will require identification of the specific E2 and E3 components of the ubiquitin cascade that affect Arf turnover.

Materials and methods

Expression plasmids

Construction of vectors expressing Arf point mutants (A1–3, A4–6, A1–6, K26R, and N-terminal variants), tagged proteins (HA, Flag), and short hairpin interfering RNAs is described elsewhere (see Supplemental Material). Human E1 cDNA was isolated as a BamH1–EcoRV fragment from pGEM7Zf(+) (Handley et al. 1991) and subcloned into the BamH1 and SnaB1 sites of pBABEpuro. The pBABEpuro-p53-ER^{TM} vector (Vater et al. 1996) was provided by Dr. Carol Vater (Immunogen, Cambridge, MA).

Cells and culture conditions

Human kidney 293T cells, mouse NIH-3T3 fibroblasts, and *Arf*-inducible MT-Arf cells (Kuo et al. 2003) were maintained in DMEM (BioWhittaker) supplemented with 10% fetal calf serum (HyClone), 4 mM glutamine, and 100 units each of penicillin and streptomycin (Life Technologies) in an 8% humidified incubator. Hamster tsBN75 and ts41 cells were maintained at 34°C in a 5% CO_2-humidified incubator (Bloom et al. 2003); MEFs were cultured as described (Zindy et al. 1998). MG132 and E64 (Calbiochem) were dissolved in DMSO prior to addition to the culture medium at 10 µM. Cells were lysed in 5 mM N-ethylmaleimide (NEM; Sigma) to inhibit ubiquitin hydrolases.

Retroviral production, infection, and cell-cycle progression

293T cells were transfected with ecotropic helper retroviral plasmid together with pSRα-MSV-tkneo vectors encoding wild-type or mutant $p19^{Arf}$ proteins (Weber et al. 2000) or with murine stem cell virus (MSCV)-internal ribosome entry site (IRES)-green fluorescent protein (GFP) vectors (Weber et al. 2000) encoding Flag-tagged wild-type or mutant human NPM proteins (Bertwistle et al. 2004). For producing VSV G pseudotyped retroviruses, 293T cells were transfected with pSRα-MSV-tkneo or pBABEpuro vectors together with pEQ-PAM3(-E) and pSRαG (Yang et al. 1995; Persons et al. 1998). Viruses harvested 24–60 h posttransfection were pooled. Exponentially growing NIH-3T3 and MT-Arf cells (2×10^5 per 10-cm-diameter culture dish) were infected once with 2 mL ecotropic virus-containing supernatant supplemented with 8 µg of polybrene (Sigma) per milliliter. MEFs and hamster cells (tsBN75 and ts41) were infected three times with 2 mL ecotropic or VSV G virus-containing supernatant, respectively, at 3-h intervals. NIH-3T3 cells infected with retroviruses encoding $p19^{Arf}$ or mutants were harvested and resuspended in solution containing propidium iodide solution, and DNA content was determined by flow cytometric analysis (Quelle et al. 1995).

Metabolic labeling and measurements of protein turnover

Following $ZnSO_4$ induction for 10 h, MT-Arf cells washed with PBS were preincubated for 30 min with leucine-free DMEM containing 10% dialyzed FBS and 4 mM L-glutamine. Cells were labeled for 2 h in the same medium with 10 µCi/mL of [3,4,5-^{3}H] L-leucine (ICN Biomedicals), washed and refed with complete medium. NIH-3T3 cells infected with pSRα retroviruses encoding $p19^{Arf}$ or mutants were labeled and chased 48 h postinfection. Where indicated, leucine-free medium was supplemented with 10 µM MG132 or DMSO alone. MEFs were starved for 30 min, labeled with 100 µCi/mL of [3,4,5-^{3}H] L-leucine and chased in complete medium as described above. Where indicated, the chase medium was supplemented with 1 µM of 4-hydroxytamoxifen (Sigma) or ethanol alone. At various times after termination of labeling, cells were lysed in RIPA buffer (50 mM Tris at pH 8.0, 150 mM NaCl, 1.0% NP-40, 0.1% SDS, 0.1% deoxycholate) containing protease inhibitors (1 mM PMSF, 0.2 U of aprotinin per mL, 10 mM β-glycerolphosphate, 1 mM NaF, and 0.1 mM NaVO4). Lysates were centrifuged at 20,000 × g at 4°C for 10 min, and soluble protein was quantified by BCA assay (Pierce). Protein (300 µg) was precipitated either with polyclonal rabbit antibody (ab80, Abcam) or rat monoclonal antibody directed against a peptide epitope comprising $p19^{Arf}$ amino acids 54–75 (see Supplemental Material). Immune complexes recovered by Protein-A Sepharose (Amersham Bioscience) and washed three times with RIPA buffer were denatured and electrophoretically separated on 4%–12% gradient Bis-Tris NuPAGE denaturing gels (Invitrogen) and transferred to PVDF membranes (Millipore). Dried membranes were coated with EN^3HANCE (PerkinElmer Life Sciences) and subjected to radiofluorography at –80°C using intensifying screens.

Immunoblotting

Procedures for immunoblotting were as described (Zindy et al. 1998). Briefly, cells were lysed in buffer containing Tween 20, and protein was quantified by BCA assay (Pierce). Proteins separated on 10% denaturing polyacrylamide or 4%–12% Bis-Tris NuPAGE gels (Invitrogen) were transferred to PVDF membranes (Millipore) and detected using antibodies to $p19^{Arf}$ (ab80; Abcam), $p14^{ARF}$ (Neomarkers), p53 (AB-7; Oncogene Research), $p21^{Cip1}$ (F-5; Santa Cruz Biotechnology), Actin (C-11; Santa Cruz Biotechnology), Flag (M2; Sigma), NPM (Zymed), and Mdm2 (2A10; provided by Arnold Levine, Institute for Advanced Study, Princeton, NJ).

To study interactions between Arf proteins and NPM, transfected 293T cells were trypsinized 48 h later and washed with PBS; cell pellets suspended in Tween-20 lysis buffer were sonicated 2 × 7 sec. Cleared lysates were precipitated for 3 h at 4°C with monoclonal antibody to mouse NPM (Zymed) or with antibodies to $p19^{Arf}$ (ab80; Abcam) followed by 2-h incubation with protein G- or protein A-Sepharose beads, respectively (Zymed). Immune complexes were washed five times in lysis buffer, boiled in 2× sample buffer, electrophoretically separated on 10% denaturing polyacrylamide gels, and transferred to PVDF membranes. Proteins were detected with monoclonal antibodies to $p19^{Arf}$ or NPM (Zymed).

In vivo ubiquitination assays

293T cells were cotransfected with 2.5 µg of MSCV retroviral Arf expression plasmid and 2.5 µg of a CMV driven HA- or His-ubiquitin plasmid (Treier et al. 1994) using Fugene-6 (Roche) according to the manufacturer's instructions. Cells treated 24 h posttransfection with either 10 µM MG132 or DMSO for 16 h were trypsinized, neutralized with complete medium, and washed with PBS. To detect HA-tagged proteins, cell pellets resuspended at 4°C in Flag lysis buffer (50 mM Tris-HCl at pH 7.4, 150 mM NaCl, 1 mM EDTA, 1% Triton X-100)

containing protease inhibitors and 5 mM NEM were disrupted by sonication (2 × 10 sec, 15% output, Virsonic 475 sonicator) and left on ice for 30 min. Lysates were centrifuged at 10,000 × g for 5 min twice, and soluble protein was quantified by BCA assay (Pierce). For immunoprecipitation of ubiquitinated Arf, lysate protein (500 µg) was diluted to 0.5 mL in RIPA buffer containing protease inhibitors. Lysates were precleared with protein G-Sepharose (Zymed) beads for 1 h, and precleared supernatants were precipitated with rat monoclonal antibody to $p19^{Arf}$ or rabbit antiserum to $p14^{ARF}$ (Novus Biologicals). Immune complexes recovered with protein G-Sepharose were washed six times with RIPA buffer and boiled in 40 µL 2× sample buffer for 5 min. Denatured immune complexes were resolved on 4%–12% gradient Bis-Tris-NuPAGE gels and transferred to PVDF membranes. Proteins were detected with antibodies to HA (3F10-HRP, Roche), $p19^{Arf}$ (Ab80, Abcam), or $p14^{ARF}$ (Neomarkers).

For purification of His-tagged ubiquitinated Arf species, cells were washed in PBS; 10% of the cell suspension was used for direct Arf immunoblotting, and the rest was resuspended in urea lysis buffer (8 M Urea, 100 mM NaH_2PO_4, 10 mM Tris-HCl at pH 8.0, 500 mM NaCl, 10% glycerol, 0.1% Triton X-100, 10 mM β-mercaptoethanol) containing 10 mM imidazole and sonicated to reduce viscosity. For protease Xa cleavage, cells (0.5 mg protein) suspended in Flag lysis buffer were incubated with 0.5 µg Xa protease (New England Biolabs) at room temperature for 12 h, and 1 mL of urea lysis buffer was added. Fifty µL Ni-NTA (QIAGEN) was added and rotated for 4 h at room temperature. Beads were washed with urea lysis buffer containing 20 mM imidazole, and His-tagged proteins were eluted twice for 20 min in 75 µL elution buffer (0.15 M Tris-HCl at pH 6.7, 5% SDS, 30% glycerol, 200 mM imidazole, 0.72 M β-mercaptoethanol). Eluted proteins were mixed with 2× sample buffer 1:1, separated on gels, transferred to PVDF membranes, and detected with monoclonal antibody to Arf.

Acknowledgments

We thank Masataka Sugimoto for the NPM constructs and for one of the ShRNA constructs; Alan Schwartz for E1 cDNA; Derek Persons for the retroviral vector encoding VSV G protein; Carol Vater for pBABEpuro $p53^{ER}$; Michele Pagano for tsBN75 cells; Rachel Neve for ts41 cells; Dirk Bohmann for the His- and HA-ubiquitin plasmids; Cam Hornsby for technical assistance; and Brenda Schulman, James Roberts, Ray Deshaies, and Richard T. Williams for suggestions during the course of this work. These studies were supported in part by NIH grant CA-71907 (M.F.R.), Cancer Center Core grant CA-21765 and by ALSAC, St. Jude Children's Research Hospital. C.J.S. and D.B. are supported by HHMI.

The publication costs of this article were defrayed in part by payment of page charges. This article must therefore be hereby marked "advertisement" in accordance with 18 USC section 1734 solely to indicate this fact.

References

Aviel, S., Winberg, G., Massucci, M., and Ciechanover, A. 2000. Degradation of the Epstein-Barr virus latent membrane protein-1 (LMP1) by the ubiquitin–proteasome pathway. Targeting via ubiquitination of the N-terminal residue. *J. Biol. Chem.* **275:** 23491–23499.

Bertwistle, D., Sugimoto, M., and Sherr, C.J. 2004. Physical and functional interactions of the Arf tumor suppressor protein with nucleophosmin/B23. *Mol. Cell. Biol.* **24:** 985–996.

Bloom, J. and Pagano, M. 2004. To be or not to be. . .ubiquitinated. *Cell Cycle* **3:** 138–140.

Bloom, J., Amador, V., Bartolini, F., DeMartino, G., and Pagano, M. 2003. Proteasome-mediated degradation of p21 via N-terminal ubiquitinylation. *Cell* **115:** 71–82.

Bradshaw, R.A., Brickey, W.W., and Walker, K.W. 1998. N-terminal processing: The methionine aminopeptidase and N^{α}-acetyl transferase families. *Trends Biochem. Sci.* **23:** 263–267.

Breitschopf, K., Bengal, E., Ziv, T., Admon, A., and Ciechanover, A. 1998. A novel site for ubiquitination: The N-terminal residue, and not internal lysines of MyoD, is essential for conjugation and degradation of the protein. *EMBO J.* **17:** 5964–5973.

Ciechanover, A. and Ben-Saadon, R. 2004. N-terminal ubiquitination: More protein substrates join in. *Trends Cell Biol.* **14:** 103–106.

Datta, A., Nag, A., and Raychaudhuri, P. 2002. Differential regulation of E2F1, DP1, and the E2F1/DP1 complex by ARF. *Mol. Cell. Biol.* **22:** 8398–8408.

David, D.C., Layfield, R., Serpell, L., Narain, Y., Goedert, M., and Spillantini, M.G. 2002. Proteasomal degradation of tau protein. *J. Neurochem.* **83:** 176–185.

Eymin, B., Karayan, L., Seite, P., Brambilla, C., Brambilla, E., Larsen, C.J., and Gazzeri, S. 2001. Human ARF binds E2F1 and inhibits its transcriptional activity. *Oncogene* **20:** 1033–1041.

Fatyol, K. and Szalay, A.A. 2001. The p14ARF tumor suppressor protein facilitates nucleolar sequestration of hypoxia-inducible factor-1α (HIF-1α) and inhibits HIF-1-mediated transcription. *J. Biol. Chem.* **276:** 28421–28429.

Handley, P.M., Mueckler, M., Siegel, N.R., Ciechanover, A., and Schwartz, A.L. 1991. Molecular cloning, sequence, and tissue distribution of the human ubiquitin-activating enzyme. *Proc. Natl. Acad. Sci.* **88:** 258–262.

Itahana, K., Bhat, K.P., Jin, A., Itahana, Y., Hawke, D., Kobayashi, R., and Zhang, Y. 2003. Tumor suppressor ARF degrades B23, a nucleolar protein involved in ribosomal biogenesis and cell proliferation. *Mol. Cell* **12:** 1151–1164.

Kamijo, T., Zindy, F., Roussel, M.F., Quelle, D.E., Downing, J.R., Ashmun, R.A., Grosveld, G., and Sherr, C.J. 1997. Tumor suppression at the mouse *INK4a* locus mediated by the alternative reading frame product $p19^{ARF}$. *Cell* **91:** 649–659.

Kamijo, T., Weber, J.D., Zambetti, G., Zindy, F., Roussel, M.F., and Sherr, C.J. 1998. Functional and physical interactions of the ARF tumor suppressor with p53 and Mdm2. *Proc. Natl. Acad. Sci.* **95:** 8292–8297.

Kim, S.H., Mitchell, M., Fujii, H., Llanos, S., and Peters, G. 2003. Absence of p16INK4a and truncation of ARF tumor suppressors in chickens. *Proc. Natl. Acad. Sci.* **100:** 211–216.

Kriwacki, R.W., Hengst, L., Tennant, L., Reed, S.I., and Wright, P.E. 1996. Structural studies of p21Waf1/Cip1/Sdi1 in the free and Cdk2-bound state: Conformational disorder mediates binding diversity. *Proc. Natl. Acad. Sci.* **93:** 11504–11509.

Kuo, M.-L., Duncavage, E.J., Mathew, R., den Besten, W., Pie, D., Naeve, D., Yamamoto, T., Cheng, C., Sherr, C.J., and Roussel, M.F. 2003. *Arf* induces p53-dependent and independent anti-proliferative genes. *Cancer Res.* **63:** 1046–1053.

Li, X. and Coffino, P. 1992. Regulated degradation of ornithine decarboxylase requires interaction with the polyamine-inducible protein antizyme. *Mol. Cell. Biol.* **12:** 3556–3562.

Liu, C.W., Corboy, M.J., DeMartino, G.N., and Thomas, P.J. 2003. Endoproteolytic activity of the proteasome. *Science* **299:** 408–411.

Martelli, F., Hamilton, T., Silver, D.P., Sharpless, N.E., Bardeesy, N., Rokas, M., DePinho, R.A., Livingston, D.M., and Grossman, S.R. 2001. p19ARF targets certain E2F species for degradation. *Proc. Natl. Acad. Sci.* **98:** 4455–4460.

Menendez, S., Khan, Z., Coomber, D.G.W., Lane, D.P., Higgins, M., Koufali, M.M., and Lain, S. 2003. Oligomerization of the human ARF tumor suppressor and its response to oxidative stress. *J. Biol. Chem.* **278:** 18720–18729.

Mori, N., Funatsu, Y., Hiruta, K., and Goto, S. 1985. Analysis of translational fidelity of ribosomes with protamine messenger RNA as a template. *Biochemistry* **24:** 1231–1239.

Nishimoto, T., Takahashi, T., and Basilico, C. 1980. A temperature-sensitive mutation affecting S-phase progression can lead to accumulation of cells with a G2 DNA content. *Som. Cell Genet.* **6:** 465–476.

Palmero, I., Pantoja, C., and Serrano, M. 1998. $p19^{ARF}$ links the tumour suppressor p53 to Ras. *Nature* **395:** 125–126.

Persons, D.A., Mehaffey, M.G., Kaleko, M., Nienhuis, A.W., and Vanin, E.F. 1998. An improved method for generating retroviral producer clones for vectors lacking a selectable marker gene. *Blood Cells Mol. Dis.* **24:** 167–182.

Petroski, M.D. and Deshaies, R.J. 2003. Context of multiubiquitin chain attachment influences the rate of Sic1 degradation. *Mol. Cell* **11:** 1435–1444.

Polevoda, B. and Sherman, F. 2003. N-terminal acetyltransferases and sequence requirements for N-terminal acetylation of eukaryotic proteins. *J. Mol. Biol.* **325:** 595–622.

Pollice, A., Nasti, V., Ronca, R., Vivo, M., Lo Iacono, M., Calogero, R., Calabro, V., and La Mantia, G. 2004. Functional and physical interaction of the human ARF tumor suppressor with Tat-binding protein-1. *J. Biol. Chem.* **279:** 6345–6353.

Quelle, D.E., Zindy, F., Ashmun, R.A., and Sherr, C.J. 1995. Alternative reading frames of the INK4a tumor suppressor gene encode two unrelated proteins capable of inducing cell cycle arrest. *Cell* **83:** 993–1000.

Quelle, D.E., Cheng, M., Ashmun, R.A., and Sherr, C.J. 1997. Cancer-associated mutations at the INK4a locus cancel cell cycle arrest by p16INK4a but not by the alternative reading frame protein p19ARF. *Proc. Natl. Acad. Sci.* **94:** 669–673.

Reinstein, E., Scheffner, M., Oren, M., Ciechanover, A., and Schwartz, A. 2000. Degradation of the E7 human papillomavirus oncoprotein by the ubiquitin–proteasome system; targeting via ubiquitination of the N-terminal residue. *Oncogene* **19:** 5944–5950.

Rocha, S., Campbell, K.J., and Perkins, N.D. 2003. p53- and Mdm2-independent repression of NF-KB transactivation by the ARF tumor suppressor. *Mol. Cell* **12:** 15–25.

Serrano, M., Hannon, G.J., and Beach, D. 1993. A new regulatory motif in cell cycle control causing specific inhibition of cyclin D/CDK4. *Nature* **366:** 704–707.

Sheaff, R.J., Singer, J.D., Swanger, J., Smitherman, M., Roberts, J.M., and Clurman, B.E. 2000. Proteasomal turnover of p21Cip1 does not require p21Cip1 ubiquitination. *Mol. Cell* **5:** 403–410.

Sherr, C.J. 2001. The *INK4a/ARF* network in tumour suppression. *Nat. Rev. Mol. Cell Biol.* **2:** 731–737.

Stott, F.J., Bates, S., James, M.C., McConnell, B.B., Starborg, M., Brookes, S., Palmero, I., Ryan, K., Hara, E., Vousden, K.H., et al. 1998. The alternative product from the human *CDKN2A* locus, $p14^{ARF}$, participates in a regulatory feedback loop with p53 and MDM2. *EMBO J.* **17:** 5001–5014.

Sugimoto, M., Kuo, M.L., Roussel, M.F., and Sherr, C.J. 2003. Nucleolar Arf tumor suppressor inhibits ribosomal RNA processing. *Mol. Cell* **11:** 415–424.

Treier, M., Staszewski, L.M., and Bohmann, D. 1994. Ubiquitin-dependent c-Jun degradation in vivo is mediated by the δ domain. *Cell* **78:** 787–798.

Vater, C.A., Bartle, L.M., Dionne, C.A., Littlewood, T.D., and Goldmacher, V.S. 1996. Induction of apoptosis by tamoxifen-activation of a p53–estrogen receptor fusion protein expressed in E1A and T24 H-ras transformed $p53^{-/-}$ mouse embryo fibroblasts. *Oncogene* **13:** 739–748.

Verma, R. and Deshaies, R.J. 2000. A proteasome howdunit: The case of the missing signal. *Cell* **101:** 341–344.

Weber, J.D., Taylor, L.J., Roussel, M.F., Sherr, C.J., and Bar-Sagi, D. 1999. Nucleolar Arf sequesters Mdm2 and activates p53. *Nat. Cell Biol.* **1:** 20–26.

Weber, J.D., Kuo, M.-L., Bothner, B., DiGiammarino, E.L., Kriwacki, R.W., Roussel, M.F., and Sherr, C.J. 2000. Cooperative signals governing ARF–Mdm2 interaction and nucleolar localization of the complex. *Mol. Cell. Biol.* **20:** 2517–2528.

Yang, Y., Vanin, E.F., Whitt, M.A., Fornerod, M., Zwart, R., Schneiderman, R.D., Grosveld, G., and Nienhuis, A.W. 1995. Inducible, high-level production of infectious murine leukemia retroviral vector particles pseudotyped with vesicular stomatitis virus G envelope protein. *Hum. Gene Ther.* **6:** 1203–1213.

Zindy, F., Quelle, D.E., Roussel, M.F., and Sherr, C.J. 1997. Expression of the $p16^{INK4a}$ tumor suppressor versus other INK4 family members during mouse development and aging. *Oncogene* **15:** 203–211.

Zindy, F., Eischen, C.M., Randle, D.H., Kamijo, T., Cleveland, J.L., Sherr, C.J., and Roussel, M.F. 1998. Myc signaling via the ARF tumor suppressor regulates p53-dependent apoptosis and immortalization. *Genes & Dev.* **12:** 2424–2433.

Zindy, F., Williams, R.T., Baudino, T.A., Rehg, J.E., Skapek, S.X., Cleveland, J.L., Roussel, M.F., and Sherr, C.J. 2003. *Arf* tumor suppressor promoter monitors latent oncogenic signals in vivo. *Proc. Natl. Acad. Sci.* **100:** 15930–15935.

N-terminal polyubiquitination and degradation of the Arf tumor suppressor

Mei-Ling Kuo, Willem den Besten, David Bertwistle, et al.

Genes Dev. 2004, **18:**
Access the most recent version at doi:10.1101/gad.1213904